

Exploiting Multi-Label Correlation in Label Distribution Learning

Zhiqiang Kou^{12*}, Jing Wang^{12*}, Yuheng Jia^{12†} and Xin Geng^{1‡}

¹ School of Computer Science and Engineering, Southeast University, Nanjing 210096, China

² MOE Key Laboratory of Computer Network and Information Integration, China
{zhiqiang_kou, wangjing91, yhjia, xgeng}@seu.edu.com,

Abstract

Label Distribution Learning (LDL) is a novel machine learning paradigm that assigns label distribution to each instance. Many LDL methods proposed to leverage label correlation in the learning process to solve the exponential-sized output space; among these, many exploited the low-rank structure of label distribution to capture label correlation. However, recent studies disclosed that label distribution matrices are typically full-rank, posing challenges to those works exploiting low-rank label correlation. Note that multi-label is generally low-rank; low-rank label correlation is widely adopted in multi-label learning (MLL) literature. Inspired by that, we introduce an auxiliary MLL process in LDL and capture low-rank label correlation on that MLL rather than LDL. In such a way, low-rank label correlation is appropriately exploited in our LDL methods. We conduct comprehensive experiments and demonstrate that our methods are superior to existing LDL methods. Besides, the ablation studies justify the advantages of exploiting low-rank label correlation in the auxiliary MLL.

Introduction

Label distribution learning (LDL) (Geng 2016) is a novel learning paradigm that provides fine-grained label information for each instance. Unlike traditional learning paradigms, LDL introduces the label description degree (Geng 2016) that is a real-value and quantify the relevance of one labels to a specific example. The label description degrees of all labels form a label distribution, which provides a comprehensive representation of labeling information. Fig.1 showcases an image from a natural-scene (Geng and Luo 2014) dataset. The average ratings are rescaled to form a label distribution $\{0.25, 0.4, 0.25, 0.1\}$, effectively capturing the varying degrees of importance assigned to labels. LDL utilizes label description degrees to effectively solve label ambiguity (Gao et al. 2017).

LDL has an overwhelming output space, which exponentially grows with the number of potential labels (Wang and Geng 2021a). To tackle this issue, label correlation has emerged as a promising solution. Many LDL works have

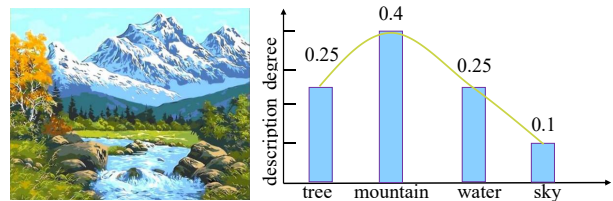


Figure 1: An image from a natural-scene dataset (Geng and Luo 2014) with a label distribution.

proposed to leverage label correlation in the learning processes. To name a few, (Xu and Zhou 2017) captured the low-rank structure of label distribution matrix to incorporate label correlation. (Jia et al. 2019) leveraged the low-rank assumption to capture label correlations shared by different groups of samples. They effectively captured label correlations in a local context. Additionally, (Ren et al. 2019) utilized a low-rank matrix to capture the global label correlation and further updated it based on different clusters to also explore local label correlations. Label correlation helps significantly improve the performance of these LDL methods. Notice that the above mentioned LDL methods assumed that label distribution has low-rank structure and relied it to exploit label correlation. However, (Wang and Geng 2021a) has demonstrated that label distribution matrices are usually full-rank, which challenges the suitability of these approaches with low-rank assumption. So, it is possible to exploit the low-rank label correlation in LDL more efficiently?

Our work is mainly inspired by two observations. The first one is that low-rank has been extensively applied to multi-label learning (MLL) to capture label correlation (Xu, Tao, and Xu 2016)(Jing et al. 2015)(Liu et al. 2021)(Wu et al. 2020)(Xu, Tao, and Xu 2016)(Yu et al. 2018). The second one is that label distribution has rich supervision information and implicitly contains multi-label information. To see that, for the example in Fig. 1 we can observe that the given label distribution contains implicit multi-labels of $\{tree, mountain, water\}$. Our basic idea is to introduce an auxiliary MLL process in LDL and exploit the low-rank label correlation on the MLL part, for example, by assuming the MLL matrix is low-rank. That is, the low-rank assumption is added on the

*These authors contributed equally.

†Corresponding author.

‡Corresponding author.

MLL part instead of the LDL part.

Following the strategy, we propose two novel LDL methods TLRLDL and TKLRLDL to exploit low-rank label correlation. First, we propose two methods to generate multi-label from label distribution. The first one utilizes a threshold to separate label distribution into multi-label, and the second one selects the top- k labels having the largest label description degrees as the positive labels. Next, we learn label distribution and the generated multi-label simultaneously, and capture the low-rank label correlation in the MLL process. We conduct expensive experiments to justify that the proposed methods outperform existing LDL approaches. Besides, the ablation studies validate the advantages of exploiting the low-rank label correlation in the MLL process. To sum up, our major contributions are as follows:

- As far as we know, this is the first work to introduce an auxiliary MLL process in LDL and exploit MLL label correlation for LDL.
- We exploit label correlation in LDL by capturing the low-rank structure in an auxiliary MLL process, which is more reasonable than directly exploiting the low-rank label correlation of LDL.
- We conduct extensive experiments to validate the advantages of our methods over existing LDL algorithms and the superiority of exploiting the low-rank label correlation in the auxiliary MLL process.

Related Work

Label Distribution Learning

As a novel learning paradigm, LDL introduces label distribution to accurately capture the degree of labeling for each instance. This unique characteristic has sparked significant research interest in the field of LDL. In this section, we provide a brief overview of the existing studies in LDL.

The existing LDL (Le et al. 2023)(Tan et al. 2023) algorithms can be broadly classified into three categories. The first category involves transforming the LDL problem into a single-label learning problem by assigning weights to the training samples. Representative algorithms in this category include PT-SVM and PT-Bayes, which utilize SVM and Bayes classifiers to solve the transformed weighted single-label learning problem. The second category focuses on adapting traditional machine learning algorithms to handle the LDL problem. For instance, the K-nearest neighbors (KNN) classifier identifies the top k neighbors of an instance and predicts the label distribution by averaging the labels of these neighbors. Back-Propagation (BP) neural networks directly optimize the descriptive degree of the final prediction through the BP algorithm. The third category comprises specialized algorithms such as IIS-LDL and BFGS-LDL. These algorithms formulate LDL as a regression problem and employ improved iterative scaling and quasi-Newton methods, respectively, to solve the regression problem efficiently. However, these LDL algorithms do not take label correlation into account.

Label Correlation in LDL

In recent years, researchers have recognized the challenge of the vast output space of LDL (Gao et al. 2017)(Wang and Geng 2019)(Shen et al. 2017)(Wang and Geng 2021b)(Ren and Geng 2017) and have developed various approaches to address this issue. These methods can be categorized into three main types: 1) global label correlation, 2) local label correlation, and 3) both global and local label correlations. In the first category, (Zhou, Xue, and Geng 2015) introduced a weighted Jeffrey’s divergence (Cha 2007) to capture label correlation by assigning weights based on the Pearson correlation coefficient. (Xu and Zhou 2017) incorporated the low-rank structure of label distribution by applying trace-norm regularization. In the second category, (Jia et al. 2019) utilized a local low-rank structure to implicitly capture the local label correlations. In the third category, (Ren et al. 2019) introduced LDL-LCLR, a method that leverages both global and local label correlations. It utilizes a low-rank matrix to capture global label correlation and updates the matrix based on different clusters to explore local label correlation.

However, many of these works rely on the assumption of low-rank to exploit label correlation. As reported by (Wang and Geng 2021a), label distribution matrix is generally full rank, which poses a challenge to those exploiting low-rank label correlation of LDL. Instead of directly exploiting low-rank label correlation of LDL, this study introduces an auxiliary MLL and exploits the low-rank label correlation on the MLL process, which can efficiently solve the above mentioned problem.

The Proposed Method

Notations: Let $\mathbf{X} = [\mathbf{x}_1, \mathbf{x}_2, \dots, \mathbf{x}_n] \in \mathbb{R}^{n \times d}$ denote the feature matrix and $\mathbf{Y} = \{y_1, y_2, \dots, y_m\}$ be the label space, where n , m , and d denote the numbers of instances, labels, and the dimension of features, respectively. The training set of the LDL is represented as $\mathbf{T} = \{(\mathbf{x}_1, \mathbf{d}_1), (\mathbf{x}_2, \mathbf{d}_2), \dots, (\mathbf{x}_n, \mathbf{d}_n)\}$, where $\mathbf{d}_i = [d_{\mathbf{x}_i}^{y_1}, d_{\mathbf{x}_i}^{y_2}, \dots, d_{\mathbf{x}_i}^{y_m}]$ is the label distribution of the i th sample \mathbf{x}_i . $d_{\mathbf{x}_i}^{y_j}$ is the label description degree of y_j to \mathbf{x}_i , which satisfies $d_{\mathbf{x}_i}^{y_j} \in [0, 1]$ and $\sum_y d_{\mathbf{x}_i}^y = 1$. The label distribution matrix is denoted as $\mathbf{D} = [\mathbf{d}_1, \mathbf{d}_2, \dots, \mathbf{d}_n] \in \mathbb{R}^{m \times n}$. LDL aims to learn a mapping function from \mathbf{T} and predict the label distribution for unseen instances.

Transforming Label Distribution into Multi-Label

This subsection will introduce two methods for transforming label distribution into multi-label. The first one is threshold-based degradation, and the second one is top- k degradation. Next, we provide details of these two methods.

Threshold-Based Multi-Label Generation To convert label distribution into multi-label, we simulate the labeling process that users typically follow when assigning labels to images or adding keywords to texts. Overall, users continue adding the most relevant labels until they perceive that the labeling is sufficiently comprehensive (Xu, Liu, and Geng 2019). Based on that, we can degrade multi-label from label distribution through this iterative labeling procedure. The process is outlined as follows:

- For each instance \mathbf{x} , find the label y_j with the highest description degree $d_{\mathbf{x}}^{y_j}$ and add it to relevant labels (i.e., $l_{\mathbf{x}}^{y_j} = 1$).
- Calculate the sum of the description degrees of all the currently relevant labels $H = \sum_{y_j \in \mathcal{Y}^+} d_{\mathbf{x}}^{y_j}$, where \mathcal{Y}^+ is the set of the currently relevant labels.
- If H is less than a predefined threshold T , continue finding the label with the highest description degree from the labels not included in \mathcal{Y} , and add it to \mathcal{Y} . Repeat this process until $H > T$.

Following this process, we can generate multi-label from label distribution that mimics the way users label data.

Top- k Based Multi-Label Generation Specifically, for any instance \mathbf{x}_i , we first sort the label description degrees in descending order. Then, we select the top- k labels with the highest label description degrees as relevant labels, and assign the remaining labels as irrelevant labels. That is, the top- k labels with the highest label description degrees are considered relevant for each instance, while the rest are deemed irrelevant.

Auxiliary MLL and Label Correlation

First, we employ the least square method to learn label distribution and minimize the L_2 -norm loss between the ground-truth label distribution and prediction, which can be formalized as the following:

$$\min_{\mathbf{W}} \frac{1}{2} \|\mathbf{W}\mathbf{X}^\top - \mathbf{D}\|_F^2 + \lambda \|\mathbf{W}\|_F^2, \quad (1)$$

where $\mathbf{W} \in \mathbb{R}^{m \times d}$ is the parameter matrix, $\|\cdot\|_F$ represents the Frobenius norm, and λ is a regularization parameter. Next, we establish the mapping relationship between label distribution and multi-label generated in the previous section. This linear mapping is formulated as:

$$\min_{\mathbf{O}} \|\mathbf{D}\mathbf{O} - \mathbf{L}\|_F^2 + \lambda \|\mathbf{O}\|_F^2, \quad (2)$$

where $\mathbf{O} \in \mathbb{R}^{n \times n}$ is the transformation parameter matrix.

Next, we exploit the low-rank label correlation. However, given the full-rank nature of the label distribution matrix, assuming a low-rank structure does not suit LDL. To address that, we encourage the low-rank structure on the MLL process, which has been widely accepted in MLL literature. That is, the predicted MLL matrix is assumed to be low-rank, which further casts Eq. (2) as:

$$\min_{\mathbf{O}} \|\mathbf{D}\mathbf{O} - \mathbf{L}\|_F^2 + \alpha \text{Rank}(\mathbf{W}\mathbf{X}^\top \mathbf{O}) + \eta \|\mathbf{O}\|_F^2, \quad (3)$$

where $\text{Rank}(\mathbf{A})$ represents the rank of \mathbf{A} , and α is a balance parameters. By jointly optimizing Problem (1) and Problem (3), we obtain the final formulation as follows:

$$\min_{\mathbf{W}, \mathbf{O}} \frac{1}{2} \|\mathbf{W}\mathbf{X}^\top - \mathbf{D}\|_F^2 + \frac{1}{2} \|\mathbf{W}\mathbf{X}^\top \mathbf{O} - \mathbf{L}\|_F^2 + \alpha \text{Rank}(\mathbf{W}\mathbf{X}^\top \mathbf{O}) + \lambda (\|\mathbf{W}\|_F^2 + \|\mathbf{O}\|_F^2), \quad (4)$$

$\text{Rank}(\mathbf{W})$ is difficult to solve due to the discrete nature of the rank function. Fortunately, as suggested by (Candès et al.

2011), the nuclear-norm (Fazel 2002) is a good surrogate for the rank function. Replacing the rank function with the nuclear-norm, we obtain the next optimization problem:

$$\min_{\mathbf{W}, \mathbf{O}} \frac{1}{2} \|\mathbf{W}\mathbf{X}^\top - \mathbf{D}\|_F^2 + \frac{1}{2} \|\mathbf{W}\mathbf{X}^\top \mathbf{O} - \mathbf{L}\|_F^2 + \alpha \|\mathbf{W}\mathbf{X}^\top \mathbf{O}\|_* + \lambda (\|\mathbf{W}\|_F^2 + \|\mathbf{O}\|_F^2). \quad (5)$$

The method learning multi-label by threshold is called TL-RLDL and the other one learning multi-label from top- k is called TKLRLDL.

Optimization

We use ADMM to solve problem (5), which is good at handling equality constraints. First, we introduce an auxiliary variable $\mathbf{G} \in \mathbb{R}^{m \times n}$ and rewrite Eq. (5) as

$$\min_{\mathbf{W}, \mathbf{O}, \mathbf{G}} \frac{1}{2} \|\mathbf{W}\mathbf{X}^\top - \mathbf{D}\|_F^2 + \frac{1}{2} \|\mathbf{W}\mathbf{X}^\top \mathbf{O} - \mathbf{L}\|_F^2 + \alpha \|\mathbf{G}\|_* + \lambda (\|\mathbf{W}\|_F^2 + \|\mathbf{O}\|_F^2) \quad (6)$$

s.t. $\mathbf{W}\mathbf{X}^\top \mathbf{O} = \mathbf{G}$.

We introduce the augmented Lagrangian function for Eq. (6)

$$\min_{\mathbf{W}, \mathbf{O}, \mathbf{G}} \frac{1}{2} \|\mathbf{W}\mathbf{X}^\top - \mathbf{D}\|_F^2 + \frac{1}{2} \|\mathbf{W}\mathbf{X}^\top \mathbf{O} - \mathbf{L}\|_F^2 + \alpha \|\mathbf{G}\|_* + \lambda (\|\mathbf{W}\|_F^2 + \|\mathbf{O}\|_F^2) + \frac{\mu}{2} \left\| \mathbf{G} - \mathbf{W}\mathbf{X}^\top \mathbf{O} - \frac{\mathbf{\Gamma}_1}{\mu} \right\|_F^2,$$

where μ is a positive penalty parameter, and $\mathbf{\Gamma}_1$ denotes the Lagrangian multipliers. It can be solved by alternately optimizing three sub-problems as follows. The whole process is summarized in Algorithm 1.

Solving G-Subproblem The subproblem w.r.t. \mathbf{G} is

$$\mathbf{G}^{k+1} = \underset{\mathbf{G}}{\text{argmin}} \alpha \|\mathbf{G}\|_* + \frac{\mu}{2} \left\| \mathbf{G} - \mathbf{W}\mathbf{X}^\top \mathbf{O} - \frac{\mathbf{\Gamma}_1}{\mu} \right\|_F^2.$$

It is a nuclear norm minimization problem and has a closed-form solution (Cai, Candès, and Shen 2010):

$$\mathbf{G}^{k+1} = S_{\alpha/\mu}(T), \quad (7)$$

where $T = \mathbf{W}\mathbf{X}^\top \mathbf{O} + \frac{\mathbf{\Gamma}_1}{\mu}$, and $S(\cdot)$ is single value thresholding operator. It first performs singular value decomposition on $\mathbf{W}\mathbf{X}^\top \mathbf{O} + \frac{\mathbf{\Gamma}_1}{\mu} = \mathbf{U}\hat{\Sigma}\mathbf{V}^\top$, and then gives the solution as $\mathbf{U}\hat{\Sigma}\mathbf{V}^\top$, where $\hat{\Sigma}_{ii} = \max(0, \Sigma_{ii} - \alpha/\mu)$.

Solving W-Subproblem The subproblem w.r.t. \mathbf{W} is

$$\mathbf{W}^{k+1} = \underset{\mathbf{W}}{\text{argmin}} \frac{1}{2} \|\mathbf{W}\mathbf{X}^\top - \mathbf{D}\|_F^2 + \frac{1}{2} \|\mathbf{W}\mathbf{X}^\top \mathbf{O} - \mathbf{L}\|_F^2 + \lambda \|\mathbf{W}\|_F^2 + \frac{\mu}{2} \left\| \mathbf{G} - \mathbf{W}\mathbf{X}^\top \mathbf{O} - \frac{\mathbf{\Gamma}_1}{\mu} \right\|_F^2$$

which is a quadratic optimization problem. The optimal solution is obtained by setting the derivative to zero and equals

$$\mathbf{W} = \left(\mathbf{X}^\top \mathbf{X} + 2\lambda + \mu \mathbf{X}^\top \mathbf{O} \mathbf{O}^\top \mathbf{X} + \mathbf{X}^\top \mathbf{O} \mathbf{O}^\top \mathbf{X} \right)^{-1} (\mu \mathbf{G} \mathbf{O}^\top \mathbf{X} - \mathbf{\Gamma}_1 \mathbf{O}^\top \mathbf{X} + \mathbf{L} \mathbf{O}^\top \mathbf{X} + \mathbf{D} \mathbf{X}) \quad (8)$$

Solving O-Subproblem The subproblem w.r.t. \mathbf{O} is

$$\begin{aligned} \mathbf{O}^{k+1} = & \frac{1}{2} \left\| \mathbf{W}\mathbf{X}^\top \mathbf{O} - \mathbf{L} \right\|_F^2 + \lambda \left\| \mathbf{O} \right\|_F^2 \\ & + \frac{\mu}{2} \left\| \mathbf{G} - \mathbf{W}\mathbf{X}^\top \mathbf{O} - \frac{\mathbf{\Gamma}_1}{\mu} \right\|_F^2 \end{aligned} \quad (9)$$

which is a quadratic optimization problem. The optimal solution is obtained by setting the derivative to zero and equals

$$\begin{aligned} \mathbf{O}^{k+1} = & \left(\mathbf{X}\mathbf{W}^\top \mathbf{W}\mathbf{X}^\top + 2\lambda + \mu \mathbf{X}\mathbf{W}^\top \mathbf{W}\mathbf{X}^\top \right)^{-1} \\ & + \left(\mathbf{X}\mathbf{W}^\top \mathbf{L} + \mu \mathbf{X}\mathbf{W}^\top \mathbf{G} - \mathbf{X}\mathbf{W}^\top \mathbf{\Gamma}_1 \right) \end{aligned} \quad (10)$$

Updating Multipliers and Penalty Parameter Finally, the Lagrange multiplier matrix and penalty parameter are updated based on following rules:

$$\begin{cases} \mathbf{\Gamma}_1^{k+1} = \mathbf{\Gamma}_1^k + \mu^k (\mathbf{G}^{k+1} - \mathbf{W}^{k+1} \mathbf{X}^\top \mathbf{O}^{k+1}) \\ \mu^{k+1} = \min(1.1\mu, \mu_{\max}) \end{cases} \quad (11)$$

where μ_{\max} is the maximum value of μ .

Algorithm 1: The proposed methods

Input: training set \mathbf{T} , parameters α, λ , and an instance \mathbf{x}

Output: prediction for \mathbf{x}

- 1: Transforming label distribution into multi-label
 - 2: Initialize $\mathbf{W}, \mathbf{O}, \mathbf{G}, \mathbf{\Gamma}_1$, and μ
 - 3: **repeat**
 - 4: Update \mathbf{G} according to Eq. (7)
 - 5: Update \mathbf{W} according to Eq. (8)
 - 6: Update \mathbf{O} according to Eq. (10)
 - 7: Update $\mathbf{\Gamma}_1$ and μ according to Eq. (11)
 - 8: **until** convergence
 - 9: **return** $\mathbf{d}^* = \mathbf{W}\mathbf{x}$.
-

Experiments

Experimental Configuration

Experimental Datasets The experiments are conducted on 16 real-world datasets with label distribution. The key characteristics of these datasets are summarized in Table 1. The first 12 datasets are collected by Geng (Geng 2016). Among these, the first eight ones (from Spoem to Alpha) are from the clustering analysis of genome-wide expression in Yeast *Saccharomyces cerevisiae* (Eisen et al. 1998). The SJAFPE is collected from JAFPE (Lyons et al. 1998), and the SBU_3DFE is obtained from BU_3DFE (Yin et al. 2006). The Gene is obtained from the research on the relationship between genes and diseases (Yu et al. 2012). The Scene consists of multi-label images, where the label distributions are transformed from rankings (Geng and Xia 2014). Besides, the SCUT-FBP, M2B, and fbp5500 are about facial beauty perception (Ren and Geng 2017). The last one RAF-ML is a facial expression dataset (Li and Deng 2019).

Evaluation Metrics We adopt six metrics to evaluate the performance of LDL methods, including Chebyshev (\downarrow), Clark (\downarrow), Kullback-Leibler (KL) (\downarrow), Canberra (\downarrow), Intersection (\uparrow), and Cosine (\uparrow) (Geng 2016). Here, \downarrow indicates that smaller values are better, and \uparrow indicates that larger values are better.

ID	Data sets	#Examples	#Features	#Labels
1	Spoem	2465	24	2
2	Spo5	2465	24	3
3	Heat	2465	24	6
4	Elu	2465	24	14
5	Dtt	2465	24	4
6	Cold	2465	24	4
7	Cdc	2465	24	15
8	Alpha	2465	24	18
9	SJAFPE	213	243	6
10	SBU-3DFE	2500	243	6
11	Gene	17892	36	68
12	Scene	2000	294	9
13	SCUT-FBP	1500	300	5
14	M2B	1240	250	5
15	fbp5500	5500	512	5
16	RAF-ML	4908	200	6

Table 1: Details of the dataset.

Comparing Methods We compare the proposed methods with seven LDL methods, including IIS-LDL, LDLLDM, EDL-LRL, IncomLDL, Adam-LDL-SCL, LCLR, and LDLLC, which are briefly introduced as follows:

- IIS-LDL (Geng 2016): It utilizes the maximum entropy model and KL divergence to learn the label distribution and does not consider label correlation.
- LDLLDM (Wang and Geng 2021a): It learns the global and local label distribution manifolds to exploit label correlations and can handle incomplete label distribution learning.
- EDL-LRL (Jia et al. 2019): It captures the low-rank structure locally when learning the label distribution to exploit local label correlations.
- IncomLDL (Xu and Zhou 2017): It utilizes trace-norm regularization and the alternating direction method of multiplier to exploit low-rank label correlation.
- Adam-LDL-SCL (Jia et al. 2021): It incorporates local label correlation by encoding it as additional features and simultaneously learns the label distribution and label correlation encoding.
- LCLR (Ren et al. 2019): It first models global label correlation using a low-rank matrix and then updates the matrix on clusters of samples to leverage local label correlation.
- LDLLC (Zheng, Jia, and Li 2018): LDLLC leverages local label correlation to ensure that prediction distributions between similar instances are as close as possible.

The parameters of the algorithms are as follows. The suggested parameters are used for IIS-LDL, EDL-LRL, LDLLC, and LDL-LCLR. For LDLLDM, λ_1, λ_2 , and λ_3 are tuned from $\{10^{-3}, \dots, 10^3\}$, and g is tuned from 1 to 14. For IncomLDL, λ is selected from the range $\{2^{-10}, \dots, 2^{10}\}$, and ρ is set to 1. For Adam-LDL-SCL, λ_1, λ_2 , and λ_3 are tuned from the set $\{10^{-3}, \dots, 10^3\}$, and

m is tuned from 0 to 14. For TLRLDL and TKLRLDL, α , λ is tuned from $\{0.005, 0.01, 0.05, 0.1, 0.5, 1, 10\}$, T is selected from 0.1 to 0.5, and k is tuned from 0 to m . We run each method for ten-fold cross-validation and tune the parameters on training set.

Results and Discussion

Table 2 presents the experimental results (mean \pm std) of the LDL algorithms on all datasets in terms of Clark, KL, and Cosine (due to limited space, the results in terms of other metrics are reported in the supplementary material), with the best results highlighted in boldface. Moreover, the last row summarized the top-one times of each method.

First, we conduct the Friedman test (Demšar 2006) to study the comparative performance among the all methods. Table 3 shows the Friedman statistics for each metric as well as the critical value. At a confidence level of 0.05, the null hypothesis that *all algorithms achieve equal performance* is clearly rejected. Next, we apply a post-hoc test, i.e., the Bonferroni-Dunn test (Demšar 2006), to compare the relative performance of TLRLDL against the other algorithms with it as the control algorithm (due to limited pages, the test results with TKLRLDL as the control algorithm are presented in the supplementary material). One algorithm is deemed to achieve significantly different performance from TLRLDL if its average rank differs from that of TLRLDL by at least one critical difference (CD) (Demšar 2006). Figure 2 illustrates the CD diagrams for each measure. In each sub-figure, if the average rank of a comparing algorithm is within one CD to that of TLRLDL, they are connected with a thick line; otherwise, it is considered to have a significantly different performance from TLRLDL.

According to Table 2, TLRLDL demonstrates remarkable performance by ranking first in 70.83% (34 out of 48) of the cases, and it achieves the best mean performance across all metrics. TLRLDL and TKLRLDL achieve the first place in 85.4% (41 out of 48) of the evaluations, which highlights the effectiveness of our methods. Besides, we can make the following observations from Figure 2:

- TLRLDL significantly outperforms IIS-LLD in terms of all metrics. This is because TLRLDL exploits label correlation, but IIS-LLD ignores label correlation, which proves the importance of label correlation for LDL.
- TLRLDL achieves significantly better performance than IncomLDL and wins ED-LRL and LCLR by a margin. These three methods all exploit low-rank label correlation in LDL which may not hold as reported in (Wang and Geng 2021a). In comparison, TLRLDL exploits low-rank label correlation in the auxiliary MLL process, which is more appropriate and suitable to LDL.
- Compared with Adam-LDL-SCL, LDLLC, and LDLLDM, TLRLDL also excels, which justifies that the low-rank label correlation on the auxiliary MLL process is a competitive way to consider label correlation for LDL.

To summarize, the experimental results validate the competitive performance of the proposed algorithms.

Ablation Study

Next, we study the advantages of exploiting the low-rank label correlation on the auxiliary MLL. First, we derive TLRLDL-a by

$$\min_{\mathbf{W}} \frac{1}{2} \|\mathbf{W}\mathbf{X}^\top - \mathbf{D}\|_F^2 + \alpha \|\mathbf{W}\mathbf{X}^\top\|_* + \lambda \|\mathbf{W}\|_F^2.$$

Second, we derive TLRLDL-b by keeping the first and fourth items of Eq. (5). That is, TLRLDL-a exploits low-rank label correlation on LDL, and TLRLDL-b ignores label correlation. We then compare TLRLDL with TLRLDL-a and TLRLDL-b.

Figure 3 presents the comparison results in terms of Clark, KL, Cosine, and Intersection. Further, we conduct the Wilcoxon signed-rank tests (Demšar 2006) for TLRLDL against TLRLDL-a and TLRLDL-b and report the results of the tests in Table 4. According to Figure 3 and Table 4, we can draw the following conclusions:

- TLRLDL and TLRLDL-a have better performance than TLRLDL-b. TLRLDL-b ignores label correlation, while TLRLDL and TLRLDL-a consider label correlation, which improves their performance. This observation further justifies the importance of label correlation for LDL.
- TLRLDL significantly outperforms TLRLDL-a. Since the different between TLRLDL and TLRLDL-a lies in that the former (the latter, respectively) exploits low-rank label correlation on MLL (LDL, respectively), this observation clearly justifies benefits of exploits low-rank label correlation on the auxiliary MLL.

Parameter Sensitivity Analysis

TLRLDL has two trade-off parameters, including α and λ . Next, we analyze the sensitivity of them.

First, we run TLRLDL with α varying from the candidate set $\{0.005, 0.01, 0.05, 0.1, 0.5, 1, 10\}$ and report its performance on SCUT-FBP, M2B, SJAFPE, SBU_3DFE, and Alpha in Figure 4. As can be seen from Figure 4, TLRLDL shows robustness w.r.t. α . As a result, we can set α to 0.1 to get satisfying performance. Likewise, we also run TLRLDL with λ ranging from the same candidate set and present its performance in Figure 4. From Figure 4, TLRLDL is robust w.r.t. λ . We may expect satisfying performance for $\lambda = 0.1$.

Conclusion

LDL has an exponential-sized output space—with a size of \mathbb{R}^m —which may decrease the performance of existing algorithms. To solve that, many LDL studies have proposed to exploit label correlation. Among these, some have proposed to exploit low-rank label correlation of label distribution, which may not hold as disclosed by (Wang and Geng 2021a) because LDL matrices are typically full-rank. To address this problem, we introduce an auxiliary MLL process in LDL and exploit low-rank label correlation on the MLL process instead of LDL. By doing this, the low-rank label correlation is implicitly exploited in our LDL methods. We conduct extensive experiments and show that our proposed

	Metric	TLRLDL	TKLRLDL	IncomLDL	IIS-LDL	EDL-LRL	Adam-LDL-SCL	LCLR	LDLLC	LDLLDM
Spoem	Clark	0.1238±.0038	0.1237±.0197	0.1314±.0028	0.1337±.0014	0.1291±.0000	0.1295±.0000	0.1302±.0001	0.1305±.0014	0.1301±.0303
	KL	0.0264±.0311	0.0249±.0032	0.0288±.1709	0.0273±.0011	0.0317±.0000	0.0318±.0000	0.0246±.0001	0.0254±.0007	0.0264±.0061
	Cosine	0.9794±.0007	0.9801±.0028	0.9769±.0239	0.9773±.0005	0.9789±.0000	0.9789±.0000	0.9783±.0003	0.9785±.0005	0.9772±.0071
Spo5	Clark	0.1769±.0810	0.1803±.0139	0.2027±.0046	0.1896±.0025	0.1853±.0000	0.1843±.0000	0.1893±.0007	0.1908±.0003	0.1860±.0390
	KL	0.0292±.0343	0.0304±.0408	0.0376±.0148	0.0336±.0008	0.0362±.0000	0.0356±.0000	0.0309±.0000	0.0314±.0000	0.0298±.0336
	Cosine	0.9759±.0213	0.9749±.0296	0.9700±.0520	0.9722±.0007	0.9738±.0000	0.9741±.0000	0.9725±.0001	0.9722±.0000	0.9737±.0301
Heat	Clark	0.1790±.0096	0.1809±.0056	0.1940±.0768	0.1998±.0014	0.1831±.0000	0.1826±.0000	0.1874±.0032	0.2717±.0064	0.1848±.0040
	KL	0.0122±.0279	0.0128±.0005	0.0146±.0141	0.0155±.0002	0.0153±.0000	0.0153±.0000	0.0130±.0003	0.0302±.0020	0.0131±.0002
	Cosine	0.9884±.0005	0.9882±.0005	0.9865±.0102	0.9855±.0002	0.9879±.0000	0.9880±.0000	0.9878±.0002	0.9695±.0022	0.9875±.0003
Elu	Clark	0.2028±.0024	0.2000±.0103	0.2325±.0612	0.2395±.0022	0.1998±.0000	0.1989±.0000	0.2032±.0028	0.4114±.0089	0.2010±.0011
	KL	0.0062±.0706	0.0063±.0138	0.0066±.0123	0.0091±.0002	0.0073±.0000	0.0072±.0000	0.0064±.0001	0.0296±.0011	0.0063±.0003
	Cosine	0.9941±.0010	0.9940±.0077	0.9918±.0049	0.9911±.0002	0.9940±.0000	0.9940±.0000	0.9938±.0001	0.9667±.0013	0.9940±.0005
Cdc	Clark	0.2142±.0719	0.2094±.0127	0.2243±.0016	0.2537±.0026	0.2168±.0000	0.2161±.0000	0.2172±.0021	0.4259±.0013	0.2147±.0309
	KL	0.0073±.0061	0.0070±.0017	0.0080±.0765	0.0099±.0002	0.0082±.0000	0.0082±.0000	0.0072±.0002	0.0291±.0001	0.0068±.0338
	Cosine	0.9935±.0263	0.9934±.0016	0.9926±.0300	0.9905±.0002	0.9933±.0000	0.9933±.0000	0.9932±.0002	0.9680±.0003	0.9934±.0463
Dtt	Clark	0.0946±.0175	0.0975±.0013	0.1039±.0188	0.1162±.0009	0.0993±.0000	0.0986±.0000	0.0971±.0006	0.1738±.0011	0.0959±.0003
	KL	0.0060±.0076	0.0062±.0008	0.0066±.0765	0.0088±.0002	0.0098±.0000	0.0098±.0000	0.0059±.0000	0.0223±.0005	0.0059±.0012
	Cosine	0.9945±.0132	0.9942±.0013	0.9933±.0300	0.9916±.0001	0.9940±.0000	0.9940±.0000	0.9943±.0000	0.9783±.0004	0.9944±.0584
Alpha	Clark	0.2072±.0042	0.2079±.0314	0.2156±.0775	0.2585±.0015	0.2107±.0000	0.2103±.0000	0.2085±.0012	0.4501±.0019	0.2116±.0236
	KL	0.0052±.0016	0.0054±.0060	0.0058±.0232	0.0084±.0001	0.0063±.0000	0.0063±.0000	0.0054±.0001	0.0267±.0002	0.0055±.0857
	Cosine	0.9948±.0015	0.9947±.0069	0.9943±.0052	0.9916±.0001	0.9946±.0000	0.9946±.0000	0.9947±.0001	0.9700±.0001	0.9946±.0362
Cold	Clark	0.1378±.0014	0.1390±.0731	0.1463±.0338	0.1568±.0014	0.1403±.0000	0.1398±.0000	0.1416±.0042	0.1512±.0040	0.1363±.0190
	KL	0.0118±.0042	0.0124±.0565	0.0139±.0056	0.0153±.0002	0.0162±.0000	0.0162±.0000	0.0128±.0009	0.0140±.0006	0.0116±.0154
	Cosine	0.9892±.0061	0.9886±.0357	0.9873±.0047	0.9855±.0003	0.9885±.0000	0.9885±.0000	0.9880±.0008	0.9866±.0005	0.9889±.0390
SJA	Clark	0.3602±.0042	0.3657±.0099	0.4567±.0061	0.4516±.0181	0.4232±.0002	1.3730±.9671	0.4049±.0082	0.4369±.0034	0.4153±.0010
	KL	0.0480±.0016	0.0518±.0277	0.0659±.0202	0.0790±.0053	0.0692±.0000	1.0106±.9024	0.0663±.0000	0.0791±.0019	0.0668±.0009
	Cosine	0.9558±.0015	0.9509±.0528	0.9321±.0187	0.9208±.0062	0.9319±.0000	0.6503±.0850	0.9372±.0000	0.9245±.0019	0.9363±.0125
SCU	Clark	1.0793±.0061	1.4568±.0000	1.5459±.0016	1.5007±.0064	1.5146±.0000	1.4654±.0000	1.3859±.0062	2.6438±.0000	1.3978±.0009
	KL	0.1779±.0015	0.1503±.0528	2.6539±.0221	0.1824±.0170	9.2314±.0504	7.4655±.0041	0.4248±.0047	16.040±.1750	0.3997±.0009
	Cosine	0.8208±.0028	0.7436±.0202	0.6108±.0689	0.6627±.0028	0.6477±.0000	0.7436±.0000	0.8126±.0011	0.5144±.0002	0.8375±.0002
SBU	Clark	0.3455±.0043	0.3520±.0016	0.3692±.0011	0.4217±.0029	0.4061±.0000	0.3718±.0000	0.3956±.0039	0.4172±.0003	0.4056±.0071
	KL	0.0502±.0857	0.0552±.0765	0.0619±.0036	0.0776±.0009	0.0726±.0000	0.0604±.0000	0.2008±.0026	0.0845±.0002	0.0791±.0370
	Cosine	0.9474±.0012	0.9449±.0300	0.9410±.0013	0.9177±.0011	0.9232±.0000	0.9367±.0000	0.9267±.0011	0.9180±.0002	0.9226±.0010
RAF	Clark	0.8652±.0082	1.4327±.0528	1.5597±.0234	1.5581±.0086	1.4495±.0003	1.4585±.0000	1.5962±.0138	1.6210±.0034	1.4151±.0016
	KL	0.0864±.18674	0.2086±.0187	6.4358±.0090	3.5105±.0654	2.2182±.0013	5.6995±.0000	13.7926±.1.8887	0.7347±.0001	0.2699±.0109
	Cosine	0.9252±.0034	0.9234±.0115	0.5631±.0101	0.7351±.0020	0.9198±.0000	0.8706±.0000	0.7968±.0047	0.6453±.0007	0.8976±.0002
M2B	Clark	1.0224±.0009	1.5160±.0023	1.4832±.0878	1.2282±.0070	1.6770±.0046	1.2093±.0000	1.6902±.1999	1.6791±.0002	1.5538±.0029
	KL	0.6972±.0108	0.7786±.0109	0.8180±.0301	0.8572±.0354	0.8632±.0044	0.8128±.0000	0.9528±.5826	0.9051±.0000	0.7556±.0083
	Cosine	0.7431±.0004	0.7786±.0070	0.7583±.0308	0.7588±.0122	0.7423±.0006	0.7639±.0000	0.5786±.0325	0.6039±.0000	0.6953±.0054
Gene	Clark	2.0077±.0041	2.1086±.0036	2.1110±.0040	2.1734±.0269	2.1102±.0000	2.1144±.0000	2.0677±.0172	2.1162±.0009	2.1374±.0036
	KL	0.2224±.0096	0.2236±.0091	0.2372±.0002	0.2380±.0069	0.2258±.0000	0.2256±.0000	0.3618±.0026	0.2374±.0054	0.2455±.0069
	Cosine	0.8387±.0028	0.8376±.0038	0.8342±.0003	0.8274±.0036	0.8347±.0000	0.8345±.0000	0.8374±.0018	0.8338±.0027	0.8290±.0021
fbp	Clark	0.5510±.0036	0.6288±.0155	1.2938±.0011	1.5065±.0023	1.6994±.0001	1.2755±.0000	1.4102±.1809	1.8756±.0857	1.2747±.0122
	KL	0.0904±.0091	0.0800±.0068	0.2017±.0003	4.2207±.0332	1.3803±.0029	0.7725±.0001	0.4208±.4110	1.7692±.4081	0.1149±.0047
	Cosine	0.9567±.0038	0.9500±.0047	0.9412±.0005	0.6572±.0017	0.7943±.0000	0.9521±.0000	0.8527±.0051	0.8242±.0123	0.9528±.0056
Sce	Clark	2.1786±.0108	2.4959±.0061	2.4765±.0303	2.4685±.0135	2.4348±.0000	2.4665±.0000	2.4230±.0025	2.4784±.0007	2.6316±.0000
	KL	2.1128±.0061	2.2857±.0015	0.2378±.0061	3.0463±.0490	2.3857±.0002	2.7001±.0000	0.8287±.0227	1.0243±.0027	4.4471±.0000
	Cosine	0.7989±.0016	0.8346±.0008	0.7297±.0071	0.6614±.0044	0.7273±.0000	0.7163±.0000	0.7290±.0042	0.6446±.0001	0.3603±.0000
top-1 times		34	7	1	0	0	0	2	0	4

Table 2: Results (mean±std) of the comparing methods in terms of three metrics (more results in terms of other three metrics are reported in the supplementary material) on 16 LDL datasets, where the best results are highlighted in boldface.

Critical Value ($\alpha = 0.05$)	Evaluation metric	Chebyshev	Clark	Canberra	KL	Cosine	Intersection
2.8500	Friedman Statistics F_F	28.0098	44.9412	46.3235	38.0000	45.7059	44.0158

Table 3: Summary of the Friedman statistics F_F in terms of six evaluation metrics, as well as the critical value at a significance level of 0.05.

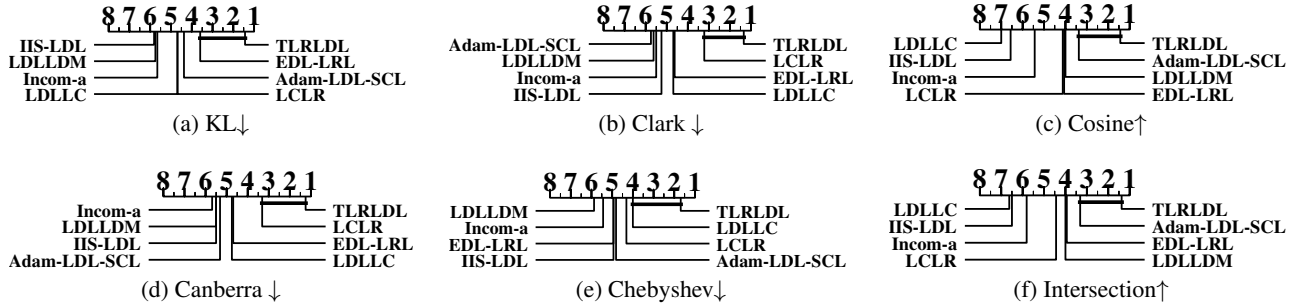


Figure 2: CD diagrams of the comparing algorithms in terms of each evaluation criterion. For the tests, CD equals 2.3296 at 0.05 significance level.

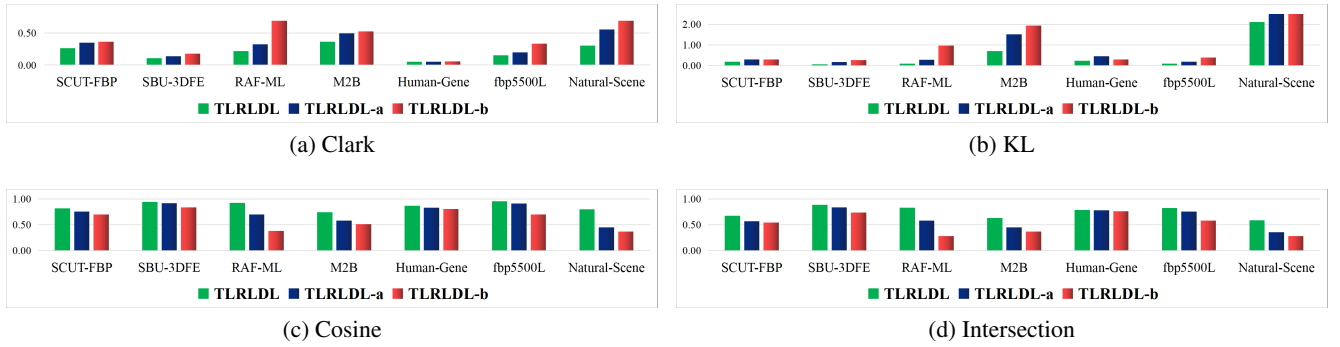


Figure 3: Ablation results on seven datasets in terms of Clark ↓, KL ↓, Cosine ↑, and Intersection ↑.

TLRLDL vs.	Chebyshev↓	Clark↓	Canberra↓	KL↓	Cosine↑	Intersection ↑
TLRLDL-a	win[4.37e-04]	win[4.38e-04]	win [4.37e-04]	win[4.46e-03]	win[4.38e-04]	win[4.38e-04]
TLRLDL-b	win[4.38e-04]	win [3.20e-03]	win[1.61e-03]	win[4.38e-04]	win [4.38e-04]	win[4.38e-04]

Table 4: The results (Win/Tie/Lose[p -value]) of the Wilcoxon signed-rank tests for TLRLDL against TLRLDL-a and TLRLDL-b at a confidence level of 0.05.

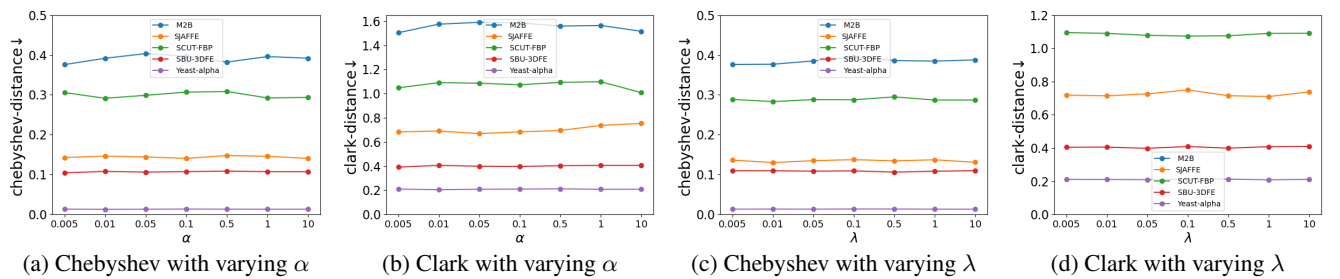


Figure 4: The performance of TLRLDL with α and λ varying from $\{0.005, 0.01, 0.05, 0.1, 0.5, 1, 10\}$ in terms of Chebyshev and Clark on SCUT-FBP, M2B, SJAFFE, SBU_3DFE, and Alpha.

methods achieve remarkably better performance than several state-of-the-art LDL methods. Moreover, further ablation studies justify the advantages of exploiting low-rank label correlation on the auxiliary MLL process.

We believe our work brings a new perspective for modeling the label correlation for LDL. In future work, we will extend our work to exploit local low-rank label correlation.

References

- Cai, J.-F.; Candès, E. J.; and Shen, Z. 2010. A singular value thresholding algorithm for matrix completion. *SIAM Journal on optimization*, 20(4): 1956–1982.
- Candès, E. J.; Li, X.; Ma, Y.; and Wright, J. 2011. Robust principal component analysis? *Journ. of the ACM*, 58(3): 1–37.
- Cha, S.-H. 2007. Comprehensive survey on distance/similarity measures between probability density functions. *City*, 1(2): 1.
- Demšar, J. 2006. Statistical comparisons of classifiers over multiple data sets. *The Journal of Machine learning research*, 7: 1–30.
- Eisen, M. B.; Spellman, P. T.; Brown, P. O.; and Botstein, D. 1998. Cluster analysis and display of genome-wide expression patterns. *Proceedings of the National Academy of Sciences*, 95(25): 14863–14868.
- Fazel, M. 2002. *Matrix rank minimization with applications*. Ph.D. thesis, PhD thesis, Stanford University.
- Gao, B.-B.; Xing, C.; Xie, C.-W.; Wu, J.; and Geng, X. 2017. Deep label distribution learning with label ambiguity. *IEEE Transactions on Image Processing*, 26(6): 2825–2838.
- Geng, X. 2016. Label distribution learning. *IEEE Transactions on Knowledge and Data Engineering*, 28(7): 1734–1748.
- Geng, X.; and Luo, L. 2014. Multilabel ranking with inconsistent rankers. In *Proceedings of the IEEE Conference on Computer Vision and Pattern Recognition*, 3742–3747.
- Geng, X.; and Xia, Y. 2014. Head pose estimation based on multivariate label distribution. In *Proceedings of the IEEE conference on computer vision and pattern recognition*, 1837–1842.
- Jia, X.; Li, Z.; Zheng, X.; Li, W.; and Huang, S.-J. 2019. Label distribution learning with label correlations on local samples. *IEEE Transactions on Knowledge and Data Engineering*, 33(4): 1619–1631.
- Jia, X.; Shen, X.; Li, W.; Lu, Y.; and Zhu, J. 2021. Label distribution learning by maintaining label ranking relation. *IEEE Transactions on Knowledge and Data Engineering*.
- Jing, L.; Yang, L.; Yu, J.; and Ng, M. K. 2015. Semi-supervised low-rank mapping learning for multi-label classification. In *Proceedings of the IEEE conference on computer vision and pattern recognition*, 1483–1491.
- Le, N.; Nguyen, K.; Tran, Q.; Tjiputra, E.; Le, B.; and Nguyen, A. 2023. Uncertainty-aware label distribution learning for facial expression recognition. In *Proceedings of the IEEE/CVF Winter Conference on Applications of Computer Vision*, 6088–6097.
- Li, S.; and Deng, W. 2019. Blended emotion in-the-wild: Multi-label facial expression recognition using crowd-sourced annotations and deep locality feature learning. *International Journal of Computer Vision*, 127(6-7): 884–906.
- Liu, W.; Wang, H.; Shen, X.; and Tsang, I. W. 2021. The emerging trends of multi-label learning. *IEEE transactions on pattern analysis and machine intelligence*, 44(11): 7955–7974.
- Lyons, M.; Akamatsu, S.; Kamachi, M.; and Gyoba, J. 1998. Coding facial expressions with gabor wavelets. In *Proceedings Third IEEE international conference on automatic face and gesture recognition*, 200–205. IEEE.
- Ren, T.; Jia, X.; Li, W.; Chen, L.; and Li, Z. 2019. Label distribution learning with label-specific features. In *IJCAI*, 3318–3324.
- Ren, Y.; and Geng, X. 2017. Sense Beauty by Label Distribution Learning. In *IJCAI*, 2648–2654.
- Shen, W.; Zhao, K.; Guo, Y.; and Yuille, A. L. 2017. Label distribution learning forests. *Advances in neural information processing systems*, 30.
- Tan, C.; Chen, S.; Geng, X.; and Ji, G. 2023. A label distribution manifold learning algorithm. *Pattern Recognition*, 135: 109112.
- Wang, J.; and Geng, X. 2019. Classification with Label Distribution Learning. In *IJCAI*, volume 1, 2.
- Wang, J.; and Geng, X. 2021a. Label distribution learning by exploiting label distribution manifold. *IEEE transactions on neural networks and learning systems*.
- Wang, J.; and Geng, X. 2021b. Label distribution learning machine. In *International Conference on Machine Learning*, 10749–10759. PMLR.
- Wu, G.; Zheng, R.; Tian, Y.; and Liu, D. 2020. Joint ranking SVM and binary relevance with robust low-rank learning for multi-label classification. *Neural Networks*, 122: 24–39.
- Xu, C.; Tao, D.; and Xu, C. 2016. Robust extreme multi-label learning. In *Proceedings of the 22nd ACM SIGKDD international conference on knowledge discovery and data mining*, 1275–1284.
- Xu, M.; and Zhou, Z.-H. 2017. Incomplete Label Distribution Learning. In *IJCAI*, 3175–3181.
- Xu, N.; Liu, Y.-P.; and Geng, X. 2019. Label enhancement for label distribution learning. *IEEE Transactions on Knowledge and Data Engineering*, 33(4): 1632–1643.
- Yin, L.; Wei, X.; Sun, Y.; Wang, J.; and Rosato, M. J. 2006. A 3D facial expression database for facial behavior research. In *7th international conference on automatic face and gesture recognition (FGR06)*, 211–216. IEEE.
- Yu, G.; Chen, X.; Domeniconi, C.; Wang, J.; Li, Z.; Zhang, Z.; and Wu, X. 2018. Feature-induced partial multi-label learning. In *2018 IEEE international conference on data mining (ICDM)*, 1398–1403. IEEE.
- Yu, J.-F.; Jiang, D.-K.; Xiao, K.; Jin, Y.; Wang, J.-H.; and Sun, X. 2012. Discriminate the falsely predicted protein-coding genes in *aeropyrum pernix* k1 genome based on graphical representation. *Match-Communications in Mathematical and Computer Chemistry*, 67(3): 845.

Zheng, X.; Jia, X.; and Li, W. 2018. Label distribution learning by exploiting sample correlations locally. In *Proceedings of the AAAI Conference on Artificial Intelligence*, volume 32.

Zhou, Y.; Xue, H.; and Geng, X. 2015. Emotion distribution recognition from facial expressions. In *Proceedings of the 23rd ACM international conference on Multimedia*, 1247–1250.